Cleveland State University
EngagedScholarship@CSU

Civil and Environmental Engineering Faculty Publications

Civil and Environmental Engineering

12-1989

Analysis of Whisker-Toughened Ceramic Components -- A Design Engineer's Viewpoint

Stephen F. Duffy PhD, PE
Cleveland State University, s.duffy@csuohio.edu

Jane M. Manderscheid

Joseph L. Palko

Follow this and additional works at: http://engagedscholarship.csuohio.edu/encee_facpub


Part of the Structures and Materials Commons

How does access to this work benefit you? Let us know!

Recommended Citation

Duffy, Stephen F. PhD, PE; Manderscheid, Jane M.; and Palko, Joseph L., "Analysis of Whisker-Toughened Ceramic Components -- A Design Engineer's Viewpoint" (1989). *Civil and Environmental Engineering Faculty Publications*. 1.
http://engagedscholarship.csuohio.edu/encee_facpub/1

This Report is brought to you for free and open access by the Civil and Environmental Engineering at EngagedScholarship@CSU. It has been accepted for inclusion in Civil and Environmental Engineering Faculty Publications by an authorized administrator of EngagedScholarship@CSU. For more information, please contact library.es@csuohio.edu.

NASA Technical Memorandum 102333

P16

Analysis of Whisker-Toughened Ceramic Components—A Design Engineer's Viewpoint

Stephen F. Duffy
Cleveland State University
Cleveland, Ohio

Jane M. Manderscheid
Lewis Research Center
Cleveland, Ohio

and

Joseph L. Palko
Cleveland State University
Cleveland, Ohio

December 1989

NASA

(NASA-TM-102333) ANALYSIS OF WHISKER-TOUGHENED CERAMIC COMPONENTS: A DESIGN ENGINEER'S VIEWPOINT (NASA) 10 p
CSCL 11D
N90-18504
Unclas
G3/24 0264339

ERRATA

NASA Technical Memorandum 102333

ANALYSIS OF WHISKER-TOUGHENED CERAMIC COMPONENTS - A DESIGN ENGINEER'S VIEWPOINT

Stephen F. Duffy, Jane M. Manderscheid, and Joseph L. Palko
December 1989

Page 7: The distributions of risk of rupture intensity depicted in figures 4 and 6 should be interchanged.

ORIGINAL CONTAINS
COLOR ILLUSTRATIONS

Analysis of Whisker-Toughened Ceramic Components—A Design Engineer's Viewpoint

Stephen F. Duffy*
Cleveland State University
Cleveland, Ohio 44115

Jane M. Manderscheid
National Aeronautics and Space Administration
Lewis Research Center
Cleveland, Ohio 44135

and

Joseph L. Palko
Cleveland State University
Cleveland, Ohio 44115

Summary

The use of ceramics components in gas turbines, cutting tools, and heat exchangers has been limited by the relatively low flaw tolerance of monolithic ceramics. The development of whisker-toughened ceramic composites offers the potential for considerable improvement in fracture toughness as well as strength. However, the variability of strength is still too high for the application of deterministic design approaches. This report reviews several phenomenological reliability theories proposed for this material system, and reports on the development of a public domain computer algorithm. This algorithm, when coupled with a general-purpose finite element program, predicts the fast fracture reliability of a structural component under multiaxial loading conditions.

Introduction

The potential advantages of ceramic matrix composites include increased fracture toughness, and creep and corrosion resistance at very high service temperatures. The primary applications under consideration are advanced turbine engine components, cutting tool bits, heat exchangers, and aerospace components (specifically those of the National Aerospace Plane). Considering that these composites will be produced from nonstrategic materials, it is not surprising that concerted research efforts are under way both in the field of materials science (to advance processing techniques) and in the field of engineering mechanics (to develop design methodologies for these material systems).

The material system of interest in this report is the whisker-toughened ceramic matrix composite. Analysis of components fabricated from this material requires a departure from the design philosophy (i.e., the factor of safety approach) prevalent in designing metallic structural components, which are more tolerant of flaws. Since failure of components fabricated from this material is governed by the scatter in strength, statistical design approaches must be used. The primary objective of this report is to review several phenomenological failure models and to report on the development of a public domain computer algorithm which, when coupled with a general-purpose finite element program, predicts the fast fracture reliability of a structural component under multiaxial loading conditions. The present version of this algorithm has been given the acronym TCARES (Toughened Ceramics Analysis and Reliability

*NASA Resident Research Associate.

Evaluation of Structures) and is a direct offspring of the CARES (a.k.a. SCARE) program (ref. 1), which has found widespread use in the design of monolithic ceramic components.

In addition to capturing the inherent scatter in strength, the reliability analysis of components fabricated from whisker-toughened ceramics must account for material symmetry imposed by whisker orientation. A noninteractive macroscopic model has been presented that accounts for the transversely isotropic material symmetry (S.F. Duffy and S.M. Arnold, Noninteractive Macroscopic Statistical Failure Theory for Whisker Reinforced Ceramic Composites, to be published in J. Compos. Mater.) often encountered in hot-pressed and injection-molded whisker-toughened ceramics. A similar model (ref. 2) has been proposed for whisker-toughened ceramics with orthotropic material symmetry. This continuum approach excludes any consideration of the microstructural events that involve interactions between individual whiskers and the matrix. Other authors have addressed fracture of ceramic matrix composites on a more local scale. A model based on probabilistic principles has been developed to compute an increased energy absorption during fracture due to whisker pull-out (ref. 3). The processes of crack deflection (ref. 4) and crack pinning (ref. 5) have also been addressed. The latter two approaches are founded in deterministic fracture mechanics. Since these crack mitigation processes strongly interact, it is difficult to experimentally detect or analytically predict the sequence of mechanisms leading to failure.

A more feasible approach is to compute reliability in terms of macrovariables by using a continuum-based criterion. This underscores a fundamental difference that exists between the materials scientist and the engineer. The materials scientist focuses on mechanisms of failure at the microstructural level, and the engineer focuses on this issue at the component level. The failure models currently incorporated into the computer algorithm TCARES adopt the engineer's viewpoint. This point of view implies that the material element under consideration is small enough to be homogeneous in stress and temperature, yet large enough to contain a sufficient number of whiskers such that the element is a statistically homogeneous continuum. This does not imply that the microscopic and macroscopic levels of focus are mutually exclusive. Indeed, a close relationship must exist between the materials scientist and the design engineer so as to develop better failure models to facilitate the use of ceramic materials in structural components.

Noninteractive Reliability Models

Here, a continuum is considered to be a chain composed of links connected in series. Therefore, the overall strength of the continuum is governed by the strength of its weakest link. It is further assumed that the events leading to failure of an individual link are not influenced by any other link in the chain. Defining f as the probability of failure of an individual link gives

$$f = \psi \, \Delta V \tag{1}$$

where ΔV denotes an increment in volume and ψ is a failure function per unit volume of material. By taking r as the reliability of an individual link, then

$$r = 1 - \psi \, \Delta V \tag{2}$$

If the failure of an individual link is considered a statistical event, and if these events are assumed to be independent, then the reliability of the continuum, denoted as R, is given as

$$R = \lim_{N \to \infty} \left\{ \prod_{\lambda=1}^{N} \left[1 - \psi(x_i) \, \Delta V \right]_{\lambda} \right\} \tag{3}$$

where N denotes the number of links and $\psi(x_i)$ is the failure function per unit volume at position x_i within the continuum. Lowercase Roman letter subscripts here and in the following expressions denote tensor indices with an implied range from 1 to 3. Greek letter subscripts and uppercase italic letters are associated with products or summations with ranges that are explicit in each expression. Alternatively, the reliability of the continuum is given by the following expression

$$R = \exp - \left(\int_V \psi \, dV \right) \tag{4}$$

where the integral within the bracket is referred to as the risk of rupture.

Depending on fabrication, a whisker-toughened composite may have isotropic, transversely isotropic, or orthotropic material symmetry. The principle of independent action (PIA) would be an appropriate first approximation macroscopic theory for isotropic whisker composites. In this instance the failure function ψ would depend only on stress or the principal invariants of stress; that is,

$$\psi = \psi(\sigma_{ij}) = \psi(\sigma_1, \sigma_2, \sigma_3) \tag{5}$$

where σ_{ij} is the Cauchy stress tensor and σ_1, σ_2, and σ_3 are the associated principal stresses.

However, for transversely isotropic whisker composites, the failure function must also reflect material symmetry. This requires that

$$\psi = \psi(\sigma_{ij}, a_i) \tag{6}$$

where a_i is a unit vector that identifies a local material orientation. This orientation, depicted in figure 1, is defined as the normal to the plane of isotropy. The sense of a_i is

ORIGINAL PAGE IS
OF POOR QUALITY

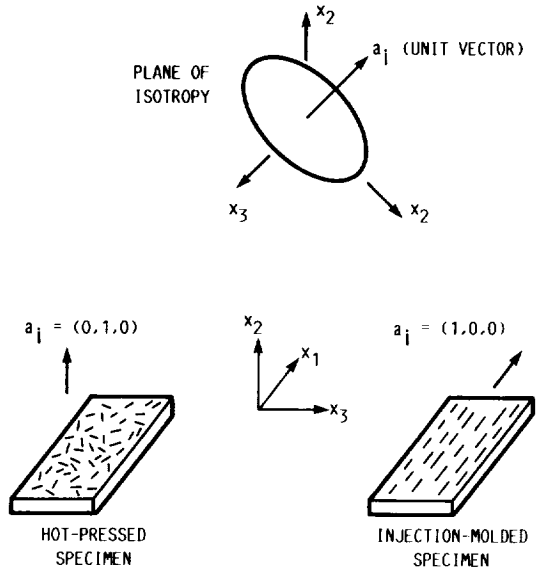

Figure 1.—Examples of transversely isotropic whisker-toughened ceramics.

TABLE I.—NONZERO MEMBERS OF INTEGRITY BASIS CORRESPONDING TO MATERIAL SYMMETRY

Material symmetry	Invariant
Isotropy	$I_1 = \sigma_{ii}$ $I_2 = \sigma_{ij}\sigma_{ji}$ $I_3 = \sigma_{ij}\sigma_{jk}\sigma_{ki}$
Transverse isotropy	$I_1 = \sigma_{ii}$ $I_2 = \sigma_{ij}\sigma_{ji}$ $I_3 = \sigma_{ij}\sigma_{jk}\sigma_{ki}$ $I_4 = a_i a_j \sigma_{ji}$ $I_5 = a_i a_j \sigma_{jk}\sigma_{ki}$
Orthotropy	$I_1 = \sigma_{ii}$ $I_2 = \sigma_{ij}\sigma_{ji}$ $I_3 = \sigma_{ij}\sigma_{jk}\sigma_{ki}$ $I_4 = a_i a_j \sigma_{ji}$ $I_5 = a_i a_j \sigma_{jk}\sigma_{ki}$ $I_6 = b_i b_j \sigma_{ji}$ $I_7 = b_i b_j \sigma_{jk}\sigma_{ki}$

immaterial, and thus its influence is taken through the product $a_i a_j$; that is,

$$\psi = \psi(\sigma_{ij}, a_i a_j) \tag{7}$$

Note that $a_i a_j$ is a symmetric second-order tensor, the trace of which satisfies the identity $a_i a_i = 1$. Furthermore, the stress and local preferred direction may vary from point to point in the continuum. Thus equation (7) implies that the stress field and the unit vector field (i.e., $\sigma_{ij}(x_k)$ and $a_i(x_k)$) must be specified to define ψ.

For orthotropic composites the failure function must also reflect the appropriate material symmetry. This requires that

$$\psi = \psi(\sigma_{ij}, a_i a_j, b_i b_j) \tag{8}$$

where a_i (a different vector than the one used for transverse isotropy) and b_i are unit vectors that identify local material orientations. These vectors are assumed to be orthogonal such that $a_i b_i = 0$.

Since ψ is a scalar valued function dependent on second-order tensors, the form of ψ must remain invariant under proper orthogonal transformations. This requires the function to be insensitive to the global coordinate system used to define the stress tensor and material directions. Through the use of invariant theory, a finite set of invariants known as an integrity basis can be developed for the isotropic, transversely isotropic, and orthotropic material symmetries (table I). The individual invariants of each integrity basis can be likened to a basis vector that helps to span a particular vector space (e.g., the set of unit vectors that span the Cartesian space). A slightly different set of invariants that correspond to physical mechanisms related to failure is constructed from each integrity basis. (See table II for a brief description of each invariant and fig. 2 for a graphical interpretation.) These invariants can be identified with a principal stress or a component of the stress tractions coincident with a material direction.

The invariants used to form ψ are assumed to act independently in producing failure such that ψ has the following general form:

$$\psi = \left(\frac{\hat{I}_1}{\beta_1}\right)^{\alpha_1} + \ldots + \left(\frac{\hat{I}_N}{\beta_M}\right)^{\alpha_M} \tag{9}$$

where $N = 3$ and $M = 1$ for isotropy, $N = 4$ and $M = 3$ for transverse isotropy, and $N = M = 5$ for orthotropy (table III). In association with each invariant, the α's correspond to Weibull shape parameters and the β's correspond to Weibull scale parameters. A variety of test methods could be used to determine these parameters. One approach is to obtain the data associated with the normal stress tractions from fast fracture of simple bend test specimens, often referred to as modulus of rupture (MOR) bars. The Weibull parameters associated with shear tractions would be obtained from appropriate shear strength tests. It is further assumed that compressive principal stresses and compressive stresses associated with a material orientation do not contribute to failure.

TCARES Algorithm

The basic data requirements of TCARES (fig. 3) closely follow the structure of its parent code CARES. The algorithm requires the stress analysis from a general-purpose finite

TABLE II.—INVARIANTS ASSOCIATED WITH PHYSICAL MECHANISMS DIRECTLY RELATED TO FAILURE

Material symmetry	Invariants used in ψ function	Comments
Isotropy	$\hat{I}_1 = \sigma_1$ $\hat{I}_1 = \sigma_2$ $\hat{I}_1 = \sigma_3$	Principal stresses; functionally dependent on the first three invariants of stress
Transverse isotropy	$\hat{I} = I_4$	Normal stress component of stress traction associated with a_i
	$\hat{I}_2 = [I_5 - (I_4)^2]^{1/2}$	Shear stress component of stress traction associated with a_i
	$\hat{I}_3 = \frac{1}{2}(I_1 - I_4) + R^a$	Maximum normal stress in plane of isotropy
	$\hat{I}_4 = \frac{1}{2}(I_1 - I_4) - R^a$	Minimum normal stress in plane of isotropy
Orthotropy	$\hat{I}_1 = I_4$	Normal stress component of stress traction associated with a_i
	$\hat{I}_2 = [I_5 - (I_4)^2]^{1/2}$	Shear stress component of stress traction associated with a_i
	$\hat{I}_3 = I_6$	Normal stress component of stress traction associated with b_i
	$\hat{I}_4 = [I_7 - (I_6)^2]^{1/2}$	Shear stress component of stress traction associated with b_i
	$\hat{I}_5 = I_1 - I_4 - I_6$	Normal stress in direction defined by cross product of a_i and b_i

[a] $R = [(\frac{1}{2})I_2 - I_5 + (\frac{1}{4})(I_4)^2 - (\frac{1}{4})(I_1)^2 + (\frac{1}{2})I_1 I_4]^{1/2}$

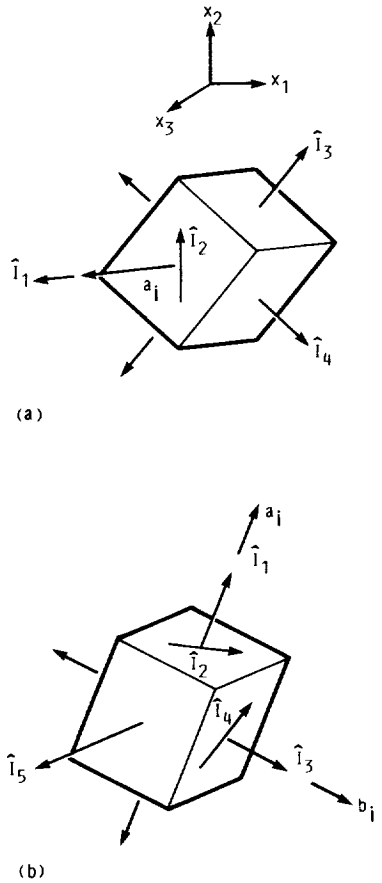

(a) Transverse isotropy.
(b) Orthotropy.

Figure 2.—Invariants associated with transverse isotropy and orthotropy.

element code. Currently, the preliminary version of TCARES is compatible with MSC/NASTRAN, although it is anticipated that future versions compatible with the MARC, ADINA, and ANSYS finite element codes will be available. The algorithm allows the user to specify temperature-dependent statistical material parameters for each material symmetry. Alternatively, the program has the capability to estimate statistical parameters from fracture data obtained from uniaxial tensile or flexural specimens. (Details of this capability can be found in ref. 6.) The preceding section on noninteractive theoretical models implies a volume flaw analytical approach. It is quite possible that the surface and volume of a structural component will fail because of distinctly different flaw populations. Accordingly the TCARES program has the capability to separately conduct surface and volume reliability analyses. The program produces as bulk output a summary of input from the finite element code, element statistical properties, element survival probabilities, and an overall component survival probability.

TCARES requires certain information from the finite element structural analysis. This includes element volumes, nodal temperatures, centroidal or nodal stresses, element principal stresses (for PIA analysis), and element identification numbers. The current version of TCARES assumes that the nodal stresses from the finite element code are provided relative to the local material orientation for transversely isotropic and orthotropic materials. This precludes having to input material orientation vectors for each finite element.

The TCARES user input requirements are grouped into three categories. (See table IV.) The first category, entitled master control input, defines control indices for stress and graphics output, the number of component materials, and information regarding the finite element code and mesh. The second

TABLE III.—FUNCTIONAL FORMS OF ψ
CORRESPONDING TO MATERIAL SYMMETRY

Material symmetry	Functional form of ψ
Isotropy $N = 3,\ M = 1$	$\psi = \left(\frac{\sigma_1}{\beta_1}\right)^{\alpha_1} + \left(\frac{\sigma_2}{\beta_1}\right)^{\alpha_1} + \left(\frac{\sigma_3}{\beta_1}\right)^{\alpha_1}$
Transverse isotropy $N = 4,\ M = 3$	$\psi = \left(\frac{I_1}{\beta_1}\right)^{\alpha_1} + \left(\frac{I_2}{\beta_2}\right)^{\alpha_2} + \left(\frac{I_3}{\beta_3}\right)^{\alpha_3} + \left(\frac{I_4}{\beta_3}\right)^{\alpha_3}$
Orthotropy $N = M = 5$	$\psi = \left(\frac{I_1}{\beta_1}\right)^{\alpha_1} + \left(\frac{I_2}{\beta_2}\right)^{\alpha_2} + \left(\frac{I_3}{\beta_3}\right)^{\alpha_3} + \left(\frac{I_4}{\beta_4}\right)^{\alpha_4} + \left(\frac{I_5}{\beta_5}\right)^{\alpha_5}$

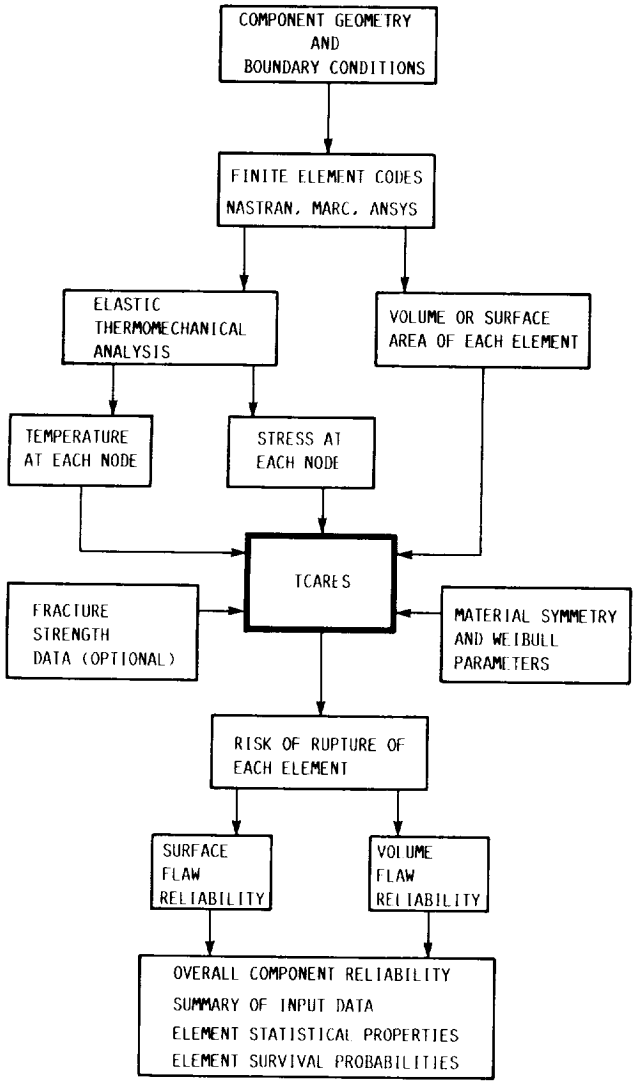

Figure 3.—Data requirements of TCARES.

category, entitled material control input, allows the user to designate the statistical parameters, and defines control indices for analysis (volume or surface) and material symmetry (isotropic, transversely isotropic, or orthotropic). The final category contains the temperature-dependent material symmetry statistical parameters. This includes the Weibull shape and scale parameters at each designated temperature.

The output from a reliability analysis conducted with TCARES can be grouped into eight broad categories. They include an echo of the master control input, a summary of element types, stress output, volume, and averaged temperature of each element. An echo of the material control indices and a summary of the analysis of each element are also provided. The latter includes material identification, failure probability, risk of rupture intensity, and the Weibull statistical parameters for each element. The program sorts and identifies 15 elements with the highest risk of rupture intensity to aid the design engineer in locating "hot" areas within a component. Finally, the overall component survival probability is given.

From Simple to Complex Geometries

Multiaxial experiments are a necessity to assess the accuracy of the noninteractive modeling approach. One experimental avenue highlighted here is the application of thermomechanical loads to tubular specimens. Initially, a thick-walled tube subjected to an applied torque is considered. A second problem is presented where the same thick-walled tube is subjected to a simultaneous application of internal pressure and axial torque. In all applications considered, isothermal conditions are assumed. However, the algorithm is capable of nonisothermal analyses if the user specifies the values of the Weibull parameters at a sufficient (and appropriate) number of temperature values. Unfortunately, at the present time no data base exists to properly characterize the multiaxial

TABLE IV.—DESCRIPTION OF INPUT PARAMETERS

Category	Input	Description
Master control input	NE	Analysis option 0—Experimental data analysis only 1—MSC/NASTRAN analysis 2—ANSYS analysis (option currently unavailable) 3—MARC analysis (option currently unavailable)
	NMATS	Number of materials for surface flaw analysis
	NMATV	Number of materials for volume flaw analysis
	IPRNT	Control index for stress and/or fracture data output 0—Suppress element stress and/or fracture data output 1—Print element stress and/or fracture data output
	IGRPH	Control index for graphics output 0—Suppress element risk of rupture intensity output 1—Print element risk of rupture intensity output
	NS	Number of cyclic symmetry segments
Temperature-independent material control input	MATID	User-designated material identification number
	ID1	Control index for experimental data analysis 1—Uniaxial tensile specimen data 2—Four point bend test data 3—All Weibull parameters specified by user 4—Censored data for suspended item analysis (uniaxial tensile specimen) 5—Censored data for suspended item analysis (four point bend test)
	ID2	Control index for material symmetry failure criteria 1—Isotropic (PIA) 2—Transversely isotropic 3—Orthotropic
	ID4	Control index for volume or surface flaw analysis 1—Volume 2—Surface
Temperature-dependent material control input	TDEG	Temperature for specified data set
	PARAM	Weibull parameters corresponding to TDEG

statistical parameters for a whisker-toughened ceramic, although efforts (ref. 7) are under way to accomplish this goal. Thus, an assessment of the program output relative to actual structural component data is reserved for a later date. For the examples that follow, Weibull statistical parameters are assumed for the purpose of illustration; however, the values adopted are well within the range of the sparse data that can be found in the open literature (refs. 8 to 10).

To test the validity of the reliability calculations performed by the program, a comparison of output with a hand calculation is presented for the aforementioned simple structural problem, that is, a thick-walled tube subjected to an axial moment or torque. It is assumed that the cylinder is fabricated from a whisker-toughened ceramic material having an orthotropic material symmetry such that $a_i = (0,0,1)$ and $b_i = (0,1,0)$ at every point in the structure. A cylindrical coordinate system readily lends itself to this application; hence, a_i is directed along the z-axis of the cylinder and b_i is oriented in the θ (circumferential) direction. With this geometry, material symmetry, and load condition, only the two terms (see table III) in the failure function associated with shear tractions are nonzero, and ψ takes the form

$$\psi = \left(\frac{Tr}{J\beta_2}\right)^{\alpha_2} + \left(\frac{Tr}{J\beta_4}\right)^{\alpha_4} \tag{10}$$

where T is the applied torque, r is the radius, and J is the polar moment of inertia. Assuming an inner radius of 1 cm, an outer radius of 5 cm, and a length of 5 cm gives

$$R = \exp\left(-\iiint \psi r \, dr \, d\theta \, dz\right)$$

$$= \exp\left(-10\pi \int \psi r \, dr\right) \tag{11}$$

ORIGINAL PAGE IS
OF POOR QUALITY

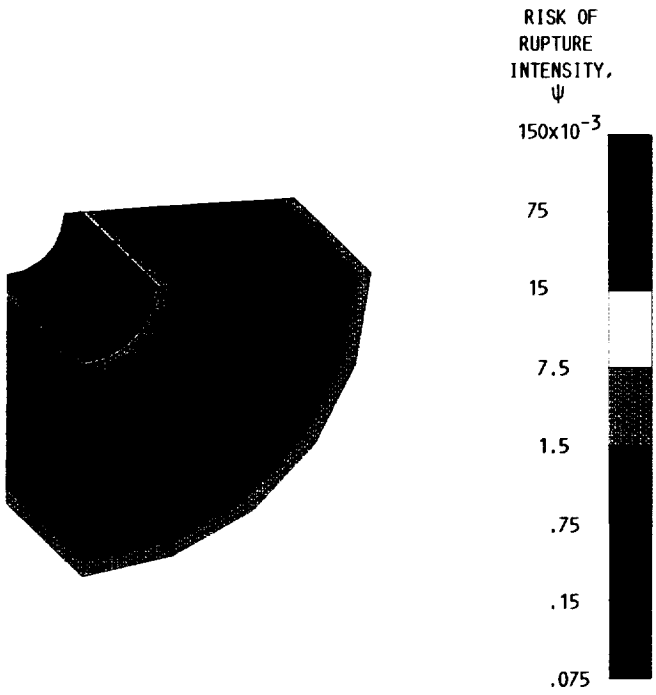

Figure 4.—Risk of rupture intensity for thick-walled tube subjected to torque of 7500 N m.

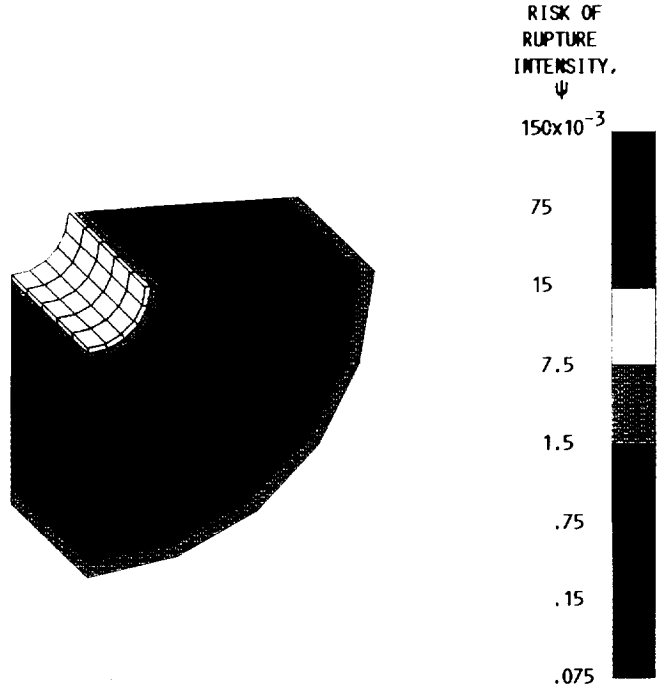

Figure 5.—Risk of rupture intensity for thick-walled tube subjected to torque of 7500 N m and internal pressure of 70 MPa.

For dimensionless reliability, the Weibull scale parameters ($\beta_1, \ldots, \beta_5$) have units of stress × (volume)$^{1/\alpha}$, and the Weibull shape parameters are unitless. With $\alpha_2 = 10$, $\beta_2 = 15\,000$, $\alpha_4 = 6.5$, $\beta_4 = 10\,000$ (the other Weibull parameters can be stipulated arbitrarily), and T = 7500 N m, the above integration yields an overall reliability of 83.6 percent. The problem was also modeled by using MSC/NASTRAN to generate a numerical solution for the stress distribution. The model was composed of 1500 eight-node elements (the stresses were within 2 percent of the closed form solution) which generated an overall component reliability of 81.8 percent. Figure 4 is a color plot of the variation of ψ in a quarter section of the component. Note that ψ (risk of rupture intensity) is a measure of reliability independent of the element geometry, and that it attains a maximum value along the outer edge of the tube.

Next, consider the same tube, subject to the conditions stated in the preceding paragraph, with an additional applied internal pressure of 70 MPa. Here α_3 and β_3 can no longer be stipulated arbitrarily and take values of $\alpha_3 = 7.5$ and $\beta_3 = 12\,000$. The overall component reliability decreases to 77.4 percent. For this load case the circumferential stress is a maximum at the inner radius, and it decreases nonlinearly through the thickness. The shear stress from the applied torque is a minimum at the inner radius, and it increases linearly with the radius. Given this multiaxial stress distribution, one expects the maximum risk of rupture intensity to occur at some point midway through the thickness. However, this is not the case, as is evident in figure 5. The maximum risk of rupture intensity

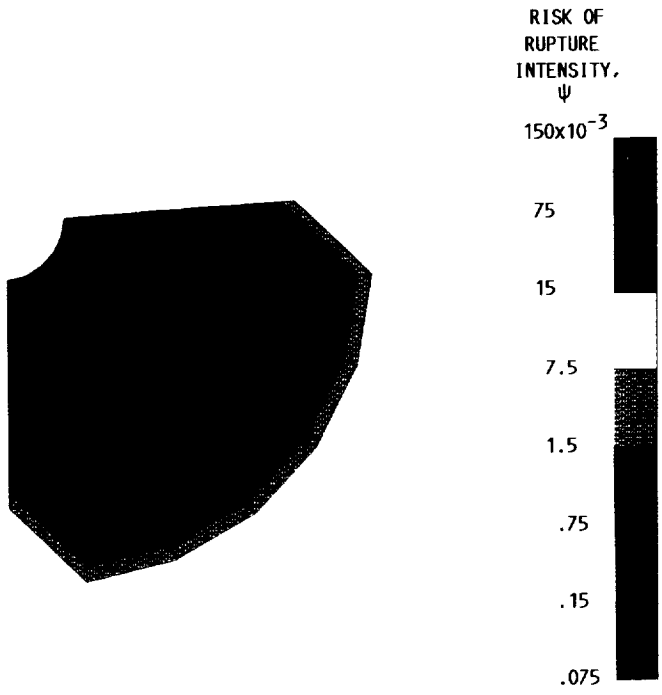

Figure 6.—Risk of rupture intensity for thick-walled tube subjected to torque of 7500 N m and internal pressure of 100 MPa.

occurs at the inner radius, and much of the inner volume of the tube remains relatively "cold." This underscores the need of not only considering overall component reliability, but also giving consideration as to where local "hot" spots occur within

a component. If this particular component were to fail, one would expect the failure to originate in the vicinity of the inner radius.

Overall component reliability can be adversely affected by either increasing the stress distribution in additional regions of the component (the so-called size effect), or by dramatically increasing the stress locally (thereby increasing the chance of failing a single link in the chain). Increasing the internal pressure of the previous example to 100 MPa sharply decreases the component reliability to 36 percent. Figure 6 depicts the variation of ψ throughout the component. It appears that the additional affected region of the component is minimal. However, ψ changes two orders of magnitude along the inner radius. Although not depicted here, the overall component reliability of the tube subjected to only an internal pressure of 100 Mpa is 44 percent, indicating that the major source in the degradation of reliability is the internal pressure.

Concluding Remarks

The applications presented here represent very straightforward structural analyses. Similar calculations and graphical interpretations can be carried over into designs with much more complex geometry and boundary conditions.

Recent advances in processing whisker-toughened ceramics have resulted in the reduction of inhomogeneities, uniform whisker distributions, and increasingly dense matrices, all of which have greatly improved the reliability of this material system. However, the variability of strength is still too high for the application of deterministic design approaches. Statistical design methodologies must be used not only to account for the scatter in ultimate strength, but also to account for decreasing bulk strength with increasing component volume (the so-called size effect). If the orientation of the whiskers is such that an anisotropic material symmetry is imparted, this must also be accounted for. Several phenomenological failure theories that take into consideration these issues in a macroscopic sense have been reviewed. In addition, a computer algorithm has been discussed that incorporates these theories and that is capable of predicting reliability given the state of stress and temperature distribution within a component.

References

1. Gyekenyesi, J.P.: SCARE: A Postprocessor Program to MSC/NASTRAN for Reliability Analysis of Structural Ceramic Components. J. Eng. Gas Turbines Power, vol. 108, no. 3, 1986, pp. 540-546.
2. Duffy, S.F.; and Manderscheid, J.M.: Noninteractive Macroscopic Reliability Model for Ceramic Matrix Composites With Orthotropic Material Symmetry. NASA TM-101414, 1989.
3. Wetherhold, R.C.: Fracture Energy for Short Brittle Fiber/Brittle Matrix Composites With Three-Dimensional Fiber Orientation. ASME Paper 89-GT-125, 1989.
4. Faber, K.T.; and Evans, A.G.: Crack Deflection Processes—I. Theory. Acta Metall., vol. 31, no. 4, 1983, pp. 565-576.
5. Lange, F.F.: The Interaction of a Crack Front With a Second-Phase Dispersion, Philos. Mag., vol. 22, 1970, pp. 983-992.
6. Nemeth, N.N.; Manderscheid, J.M.; and Gyekenyesi, J.P.: Ceramic Analysis and Reliability Evaluation of Structures (CARES)—User's and Programmer's Manual. NASA TP-2916, 1989.
7. Shaw, N.J.; and Bubsey, R.T.: Toughened Ceramics Life Prediction. NASA proposal submitted to Oak Ridge National Laboratory—Ceramic Technology for Advanced Heat Engines Project, 1987.
8. Claussen, H.; and Petzow, G.: Whisker-Reinforced Zirconia Toughened Ceramics. Tailoring Multiphase and Composite Ceramics; Proceedings of the 21st University Conference on Ceramic Science, Plenum Press, New York, 1985, pp. 649-662.
9. Tiegs, T.N.; and Becher, P.F.: Alumina-SiC Whisker Composites: Application to Heat Engines. Presented at the 23rd Automotive Technology Development Contractors' Coordination Meeting, Dearborn, MI, 1985.
10. Rhodes, J.F., et al.: Ceramic Reinforced Ceramics. PM Aerospace Materials; Proceedings of the International Conference, Volume I, MPR Publishing, Shrewsbury, England, 1984, pp. 43-1 to 43-22.

NASA
National Aeronautics and Space Administration

Report Documentation Page

1. Report No.	2. Government Accession No.	3. Recipient's Catalog No.
NASA TM-102333		

4. Title and Subtitle	5. Report Date
Analysis of Whisker-Toughened Ceramic Components—A Design Engineer's Viewpoint	December 1989
	6. Performing Organization Code

7. Author(s)	8. Performing Organization Report No.
Stephen F. Duffy, Jane M. Manderscheid, and Joseph L. Palko	E-5042
	10. Work Unit No. 778-32-11

9. Performing Organization Name and Address	11. Contract or Grant No.
National Aeronautics and Space Administration Lewis Research Center Cleveland, Ohio 44135-3191	
	13. Type of Report and Period Covered Technical Memorandum

12. Sponsoring Agency Name and Address	14. Sponsoring Agency Code
National Aeronautics and Space Administration Washington, D.C. 20546-0001	

15. Supplementary Notes

Stephen F. Duffy and Joseph L. Palko, Cleveland State University, Dept. of Civil Engineering, Cleveland, Ohio 44115; Stephen F. Duffy, NASA Resident Research Associate. Jane M. Manderscheid, NASA Lewis Research Center.

16. Abstract

The use of ceramics components in gas turbines, cutting tools, and heat exchangers has been limited by the relatively low flaw tolerance of monolithic ceramics. The development of whisker-toughened ceramic composites offers the potential for considerable improvement in fracture toughness as well as strength. However, the variability of strength is still too high for the application of deterministic design approaches. This report reviews several phenomenological reliability theories proposed for this material system, and reports on the development of a public domain computer algorithm. This algorithm, when coupled with a general-purpose finite element program, predicts the fast fracture reliability of a structural component under multiaxial loading conditions.

17. Key Words (Suggested by Author(s))	18. Distribution Statement
Composites; Whiskers; Ceramics; Reliability; Weibull analysis; Finite element analysis	Unclassified – Unlimited Subject Category 24

19. Security Classif. (of this report)	20. Security Classif. (of this page)	21. No of pages	22. Price*
Unclassified	Unclassified	9	A02

*For sale by the National Technical Information Service, Springfield, Virginia 22161